ChemComm

RSC Publishing

COMMUNICATION

View Article Online
View Journal | View Issue

A face-capped $[Fe_4L_4]^{8+}$ spin crossover tetrahedral cage†

Cite this: *Chem. Commun.*, 2013, **49**, 1597

Received 26th October 2012,
Accepted 8th January 2013

DOI: 10.1039/c3cc00012e

www.rsc.org/chemcomm

Alan Ferguson,*[a] Marie A. Squire,[a] Diana Siretanu,[bc] Dmitri Mitcov,[bc] Corine Mathonière,[de] Rodolphe Clérac*[bc] and Paul E. Kruger*[a]

Reported here is a face-capped Fe(II) molecular tetrahedron, $[Fe_4L_4](BF_4)_8$, 1. Single crystal X-ray diffraction at 153 and 293 K suggest spin crossover (SCO) and variable temperature magnetic susceptibility measurements confirm 1 displays thermally driven SCO behaviour in the solid state and in dilute acetone solution centred around 284–288 K.

The synthesis of molecular cages through self-assembly has produced an impressive variety of species, many of which are capable of encapsulating guest molecules within their internal cavities.[1] Taking advantage of this host–guest behaviour has allowed these capsules to catalyse reactions,[2] protect otherwise unstable molecules[3] and selectively bind guests within their cavities.[4] Some of the best studied examples are the tetrahedral molecular cages.[5] These are typically of the form $[M_4L_6]$[6] or $[M_4L_4]$[7] where the ligands, **L**, form the edges or faces, respectively, of the tetrahedron. Impressive as these examples are, to date, none have demonstrated the ability to SCO under the influence of an external perturbation.

The remarkable host–guest properties of molecular cages inspired us to explore the possibility of incorporating Fe(II) SCO centres into these nano-capsules. Materials displaying SCO behaviour continue to be intensively studied due to their potential use as the active components within memory, display and sensing devices.[8] SCO in Fe(II) complexes with octahedral geometry is particularly obvious as it transforms a diamagnetic low-spin state ($S = 0$) to a paramagnetic high-spin state ($S = 2$) with striking parallel change in colour and notable expansion of the Fe(II) coordination sphere. SCO has been observed in a wide range of discrete complexes,[9] polymeric and network species.[10] Variation of the ligands or constituents within the crystal lattice in these systems can significantly affect the magnetic properties allowing SCO behaviour to be tuned.[11]

Despite the fascinating link between host–guest and SCO behaviour, the synthesis of a SCO nano-capsule capable of binding guests is so far limited to one example.[12] An impressive 'nano-ball' shows partial SCO in the solid state and has a large 3 nm cavity filled by solvent molecules. These guest molecules can be removed reversibly to alter the magnetic properties of the complex. Here we report the assembly of a nano-scale molecular spin-switching tetrahedron $[Fe_4L_4]^{8+}$, which shows a striking magnetic response to a range of external stimuli, including temperature and solvent molecules. Of particular note is the abrupt cooperative SCO observed in dilute acetone solution.

To create a SCO tetrahedral cage we combined, in MeCN solution, $Fe(BF_4)_2$ with the ligand sub-components: 2,4,6-tris(4-aminophenoxy)-triazine and 2-imidazolecarboxaldehyde in 4 : 4 : 12 stoichiometry, respectively. Ligand self-assembly about Fe(II) centres form the pseudo-C_3-symmetric tris-imine ligand, **L**, capable of occupying the faces of the resultant $[Fe_4L_4]^{8+}$ tetrahedron (Fig. S1–S3, ESI†). We have previously shown that imino-imidazole type ligands provide the appropriate ligand field strength about Fe(II) to allow SCO.[13] When all the reactants were combined, the MeCN solution became dark red in colour which, following the slow diffusion of benzene over several days, produced large deep red rod-like crystals.

Mass spectrometry of these crystals re-dissolved in acetone solution revealed a series of peaks of various charges that may be assigned to $\{[Fe_4L_4]^{n+}[BF_4]^-\}$ (n = 4–7) species. It is evident that the charged species are generated by the loss of seven $[BF_4]^-$ ions (with the retention of one $[BF_4]^-$ ion) and the subsequent removal of 1, 2, 3 or 4 imidazole H-atoms to give +6, +5, +4 and +3 charged species, respectively (Fig. S4 and S5, ESI†). Notable from these data is the persistent presence of one $[BF_4]^-$ ion, which we suspect is located within the tetrahedron's cavity. The ^{19}F NMR spectrum at 298 K shows two different locations for the $[BF_4]^-$ ions, with the signals at −147 and −157 ppm assigned to 'free' and encapsulated $[BF_4]^-$ ions, respectively (Fig. S6, ESI†).[14] The ^1H NMR spectrum showed pronounced peak broadening and shifting at 298 K consistent with paramagnetic Fe(II) (Fig. S7, ESI†).[15]

Single crystal X-ray diffraction at 153 K confirmed the formation of $[Fe_4L_4]^{8+}$ (Fig. 1). The structure of $\{[Fe_4L_4](BF_4)_8 \cdot 14.75MeCN \cdot 4.5C_6H_6 \cdot 3H_2O\}$, **1**, was refined in the monoclinic space group

[a] *Department of Chemistry, University of Canterbury, Private Bag 4800, Christchurch, 8041, New Zealand. E-mail: paul.kruger@canterbury.ac.nz*
[b] *CNRS, CRPP, UPR 8641, F-33600 Pessac, France*
[c] *Univ. of Bordeaux, CRPP, UPR 8641, F-33600 Pessac, France. E-mail: clerac@crpp-bordeaux.cnrs.fr*
[d] *CNRS, ICMCB, UPR 9048, F-33600 Pessac, France*
[e] *Univ. of Bordeaux, ICMCB, UPR 9048, F-33600 Pessac, France*

† Electronic supplementary information (ESI) available: Synthesis and characterization of **L**, synthesis and characterization of **1**, TGA, UV-vis. data, ^{19}F and ^1H NMR spectra, additional magnetic, optical and photo-magnetic data, and CIF files for **1**. CCDC 907705 and 907706. For ESI and crystallographic data in CIF or other electronic format see DOI: 10.1039/c3cc00012e

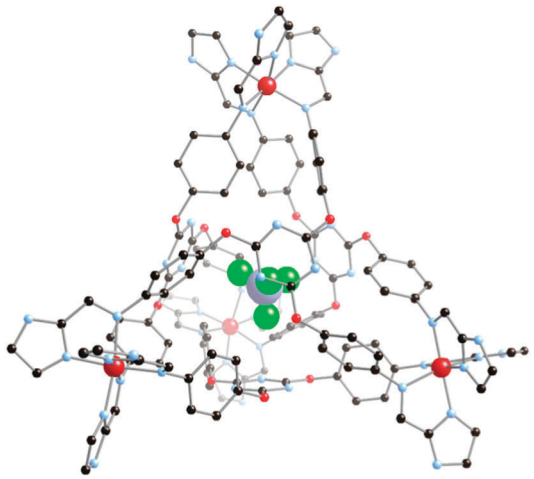

Fig. 1 Crystal structure of **1** at 153 K, showing the encapsulated $[BF_4]^-$ anion in space-filling mode. All hydrogen atoms, solvent molecules and lattice anions have been removed for clarity.

*C*2/*c* (Table S1, ESI†). As anticipated, the four ligands, **L**, occupy the faces of the $[Fe_4L_4]^{8+}$ tetrahedron, with coordination of three imino-imidazole functionalities about each of the four Fe(II) centres, which occupy the vertices of the tetrahedron. The three ligand arms radiate from the central triazine ring such that in a given tetrahedron they all either twist to the left (as shown in Fig. 1) or to the right (in an adjacent complex). A given tetrahedron is either of *Λ*,*Λ*,*Λ*,*Λ* or *Λ*,*Λ*,*Λ*,*Λ* chirality at the Fe(II) centres, with adjacent tetrahedra being of opposite chirality. There are two crystallographically distinct Fe(II) centres within the tetrahedron. Inspection of the Fe–N bond distances for Fe1 (1.952(5)–2.013(5) Å) and for Fe2 (1.942(6)–2.017(6) Å), indicates that they are similar and that all Fe(II) centres are in their low spin state at 153 K. The average Fe–Fe separation within the tetrahedron is 14.16 Å and the internal cavity volume is 106 Å^3 (Fig. S8, ESI†).[16] This volume is smaller than that observed for other tetrahedra with similar metal–metal distances when the ligands form the edges of the tetrahedron $[M_4L_6]$ (*ca.* 141 Å^3)[6] or face-capped tetrahedra featuring rigid ligands $[M_4L_4]$ (*ca.* 229 Å^3).[7] This smaller volume is probably due to the twisting of the flexible arms of the ligand resulting in the phenyl rings being directed into the cavity and thus reducing its volume.

Located at the centre of the cavity is one $[BF_4]^-$ ion. Each fluorine atom is directed towards the centre of a triazine ring on the face of the tetrahedron with F···centre-of-ring distances of *ca.* 3.0 Å indicative of strong interaction.[17] Indeed, these F···π interactions may template the self-assembly of the cage. The remaining seven [BF4]$^-$ anions are decorated around the imidazole head groups on the periphery of the cage. These anions act as hydrogen bond acceptors for the imidazole N–H donors, and lead to the formation of an extensive hydrogen bonded network throughout the crystal lattice allowing each cage to interact with ten neighbouring cages.

Despite the instability of crystals of **1** due to solvent loss (Fig. S9, ESI†), a diffraction dataset on a single crystal of **1** sealed within a capillary tube was also collected at 293 K (Table S1, ESI†). While the data collected was extremely weak, it was of sufficient quality to allow determination of the structure and to again identify the tetrahedral cage with associated $[BF_4]^-$ ions and solvent molecules. The data were solved within the same crystal system although the unit cell parameters all increase significantly with the most striking changes in the *c*-edge length, which has increased by ~7% (*viz.* 37.854(3)–40.415(5) Å) and the *β*-angle which opens up by ~3% (*viz.* 123.814(9)–127.15(2)°). The combination of these changes results in a ~5% increase in the cell volume, which is consistent with partial SCO of the complex.[15] Most notably; the cavity volume has increased by 7.5%. The Fe–N bond distances also support the onset of SCO in **1**. While the $Fe–N_{imidazole}$ bond lengths for Fe1 remain almost constant the $Fe–N_{imine}$ bond lengths increase (average increases from 2.002 Å to 2.076 Å), as do each of the Fe–N bond distances around Fe2 (average Fe–N increase from 1.979 Å to 2.062 Å, Table S2, ESI†).

To further study the SCO behaviour of **1**, dc magnetic susceptibility measurements were performed. Only data below 290 K are reported for the freshly isolated sample of **1** (black open dots, Fig. 2) as above this temperature, solvent loss is evident on the magnetic susceptibility in agreement with TGA data (Fig. S9, ESI†). At 290 K, the χT product is 7.4 cm^3 K mol^{-1}, which is lower than the expected value for four $S = 2$ high spin Fe(II) ions (C = 12–13 cm^3 K mol^{-1} with g = 2.0–2.1), suggesting that the cage is ~60% high-spin at this temperature. The χT product gradually decreases as the sample is cooled and the SCO is complete at ~120 K leading to a complete low-spin state for the cage with a small residual paramagnetic signal (at 60 K: 0.15 cm^3 K mol^{-1}) observed. Modelling the χT *vs.* T data of **1** using the ideal solution model produced a best fit with the following parameters: ΔH = 14.1 kJ mol^{-1}; $T_{1/2}$ = 284 K; ΔS = 50.3 J K^{-1} mol^{-1}.[18]

Quite remarkably, when **1** is diluted in acetone, the SCO properties probed by magnetic susceptibility are clearly retained. As shown in Fig. 2 (blue squares), the χT product of this solution is 10.1 cm^3 K mol^{-1} at 300 K and exhibits a complete low-spin state below 220 K. The ideal solution model is also able to reproduce the experimental data with a slightly higher $T_{1/2}$, 288 K, and significantly larger thermodynamic parameters than in solid state: ΔH = 57.4 kJ mol^{-1} and ΔS = 199 J K^{-1} mol^{-1} (Fig. 2).[18] This result is probably caused by the higher symmetry of the tetrahedron in solution and thus a more degenerate paramagnetic state.[19]

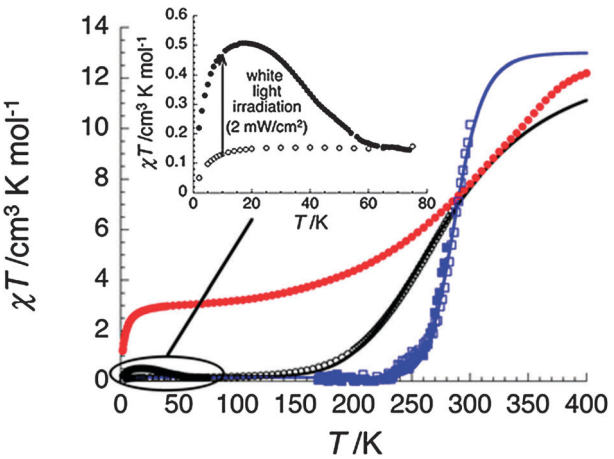

Fig. 2 χT *vs.* T data for **1** (with χ defined as molar magnetic susceptibility and equal to M/H per tetrahedron) in solvated crystals of **1** (open and full black dots, before and after white light irradiation respectively; inset: expanded view of the low temperature region below 80 K). After drying **1** at 100 °C during 24 h (red dots) and in a diluted acetone solution (full and open blue squares in cooling and heating modes respectively) at *ca.* 0.4 K min^{-1} and 1 T; solid lines are fits to the ideal solution model.[18]

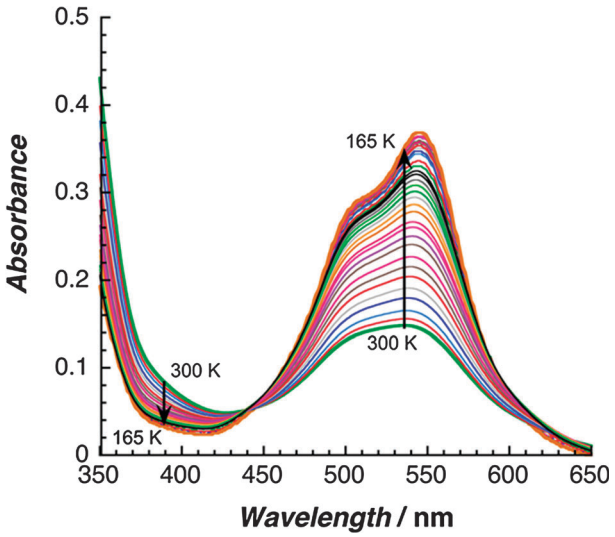

Fig. 3 UV-vis spectra for **1** in acetone (1.06×10^{-4} mol L^{-1}) in cooling mode from 300 K to the freezing point of the solution (at 0.2 to 0.3 K min^{-1}).

The SCO of **1** in solution was further probed through variable temperature UV-Vis spectroscopy (Fig. 3 and Fig. S14, ESI†). Indicative changes within the UV-Vis spectra on decreasing temperature (+27 to −108 °C), are the increase in intensity of characteristic broad absorption MLCT bands at 502 nm and 545 nm ($t_2 \rightarrow \pi^*$) and the decrease in the intra-ligand band at 335 nm ($\pi \rightarrow \pi^*$), in line with the formation of the low spin state at lower temperature.

The magnetic susceptibility of a dried sample of **1** was also measured allowing measurements up to 400 K (red trace, Fig. 2). The χT product at 400 K is 12.4 cm^3 K mol^{-1}, however the shape of the χT curve suggests the cage is not quite in its complete high-spin state even at this elevated temperature. As the temperature is lowered the χT product again gradually decreases before reaching a plateau at ~60 K. The χT product at 60 K is 3.08 cm^3 K mol^{-1} suggesting that one Fe(II) centre remains in the high-spin state. Below 10 K the decrease in the χT product is due to the well-known zero field splitting of the HS Fe(II) centre. Fitting of χT *vs.* T data for the dried sample using the same model[18] as above was not possible, probably due to the different thermal SCO behaviour of the individual Fe(II) centres.

Optical reflectivity and photomagnetic properties of **1** were also investigated (Fig. S10–S13, ESI†). Both types of measurements revealed a weak photo-sensitivity of the compound. At 10 K, a small photomagnetic effect under white-light irradiation of 2 mW cm^{-2} is detected as shown by the χT product that increases from 0.13 to around 0.46 cm^3 K mol^{-1} after 17 hours (Fig. 2 and Fig. S13, ESI†). Increasing the temperature at 0.4 K min^{-1}, the photo-induced high-spin species relax to their thermodynamic low-spin state around 60 K. The photo-induced high-spin species are probably located in a small volume of sample close to its surface. Attempts to access to the fully high-spin state of **1** at 10 K using irradiation at different wavelengths and powers were unsuccessful.

In conclusion, **1** represents the first example of a molecular tetrahedron showing SCO behaviour in the solid state and strikingly in dilute solution. These initial results highlight the potential of guest occupied molecular cages as SCO materials and suggest that many of the previously reported molecular cages could be converted to show SCO behaviour. Tuning of the SCO should be possible through careful manipulation of the central ligand, the coordinating group and the guest molecule. Studies on the effect of the guest molecule are of particular interest due to the potential to create a guest induced SCO material. As such an investigation into the host–guest behaviour of **1** is underway, the results of which will be published in due course. These results also potentially augur well for the controlled capture and release of encapsulated guests under the influence of external stimuli that switch SCO (*e.g.* T, light, pressure *etc.*). These goals form the basis of our ongoing research.

This work was supported by the Marsden Fund, the CNRS, the University of Bordeaux, the Conseil Régional d'Aquitaine (GIS Advanced Materials in Aquitaine/COMET Project), and Erasmus Mundus ECW Program PhD fellowships to D.S. and D.M.

Notes and references

1 D. J. Cram, *Nature*, 1992, **356**, 29; M. Fujita, D. Oguro, M. Miyazawa, H. Oka, K. Yamaguchi and K. Ogura, *Nature*, 1995, **378**, 469; M. Yoshizawa, J. K. Klosterman and M. Fujita, *Angew. Chem., Int. Ed.*, 2009, **48**, 3418; S. J. Dalgarno, N. P. Power and J. L. Atwood, *Coord. Chem. Rev.*, 2008, **252**, 825; M. D. Ward, *Chem. Commun.*, 2009, 4487.
2 M. Yoshizawa, M. Tamura and M. Fujita, *Science*, 2006, **312**, 251; M. D. Pluth, R. G. Bergman and K. N. Raymond, *Science*, 2007, **316**, 85.
3 P. Mal, B. Breiner, K. Rissanen and J. R. Nitschke, *Science*, 2009, **324**, 1697; M. Yoshizawa, T. Kusukawa, M. Fujita and K. Yamaguchi, *J. Am. Chem. Soc.*, 2000, **122**, 6311.
4 W. Meng, B. Breiner, K. Rissanen, J. D. Thoburn, J. K. Clegg and J. R. Nitschke, *Angew. Chem., Int. Ed.*, 2011, **50**, 3479.
5 A. J. Amoroso, J. Jeffery, P. Jones, J. McCleverty, P. Thornton and M. D. Ward, *Angew. Chem., Int. Ed. Engl.*, 1995, **34**, 1443; J. K. Clegg, F. Li, K. A. Jolliffe, G. V. Meehan and L. F. Lindoy, *Chem. Commun.*, 2011, **47**, 6042.
6 C. R. K. Glasson, J. K. Clegg, J. C. McMurtie, G. V. Meehan, L. F. Lindoy, C. A. Motti, B. Moubaraki, K. S. Murray and J. D. Cashion, *Chem. Sci.*, 2011, **2**, 540; I. A. Riddell, M. M. J. Smulders, J. K. Clegg and J. R. Nitschke, *Chem. Commun.*, 2011, **47**, 457.
7 R. A. Bilbeisi, J. K. Clegg, N. Elgrishi, X. D. Hatten, M. Devillard, B. Breiner, P. Mal and J. R. Nitschke, *J. Am. Chem. Soc.*, 2012, **134**, 5110.
8 O. Kahn and C. J. Martinez, *Science*, 1998, **279**, 44.
9 Z. Ni and M. P. Shores, *J. Am. Chem. Soc.*, 2009, **131**, 32; K. E. Funck, A. V. Prosvirin, C. Mathonière, R. Clérac and K. R. Dunbar, *Inorg. Chem.*, 2011, **50**, 2782; R. Wei, Q. Huo, J. Tao, R. Huang and L. Zheng, *Angew. Chem., Int. Ed.*, 2011, **50**, 8940; D. Wu, O. Sato, Y. Einaga and C. Duan, *Angew. Chem., Int. Ed.*, 2009, **48**, 1475.
10 Y. Garcia, V. Niel, M. C. Muñoz and J. A. Real, *Top. Curr. Chem.*, 2004, **233**, 229; G. J. Halder, C. J. Kepert, B. Moubaraki, K. S. Murray and J. D. Cashion, *Science*, 2002, **298**, 1762; S. M. Neville, G. J. Halder, K. W. Chapman, M. B. Duriska, B. Moubaraki, K. S. Murray and C. J. Kepert, *J. Am. Chem. Soc.*, 2009, **131**, 12106.
11 P. Gütlich, Y. Garcia and H. A. Goodwin, *Chem. Soc. Rev.*, 2000, **29**, 419; M. A. Halcrow, *Chem. Soc. Rev.*, 2011, **40**, 4119.
12 M. B. Duriska, S. M. Neville, B. Moubaraki, J. D. Cashion, G. J. Halder, K. W. Chapman, C. Balde, J.-F. Létard, K. S. Murray, C. J. Kepert and S. R. Batten, *Angew. Chem., Int. Ed.*, 2009, **48**, 2549.
13 R. J. Archer, C. S. Hawes, G. N. Jameson, V. McKee, B. Moubaraki, N. F. Chilton, K. S. Murray, W. Schmitt and P. E. Kruger, *Dalton Trans.*, 2011, **40**, 12368; D. Pelleteret, R. Clérac, C. Mathonière, E. Harté, W. Schmitt and P. E. Kruger, *Chem. Commun.*, 2009, 221; J. R. Thompson, R. J. Archer, C. S. Hawes, A. Ferguson, A. Wattiaux, C. Mathonière, R. Clérac and P. E. Kruger, *Dalton Trans.*, 2012, **41**, 12720.
14 R. L. Paul, S. P. Argent, J. C. Jeffery, L. P. Harding, J. M. Lynam and M. D. Ward, *Dalton Trans.*, 2004, 3453.
15 E. Breuning, M. Ruben, J.-M. Lehn, F. Renz, Y. Garcia, V. Ksenofontov, P. Gütlich, E. Wegelius and K. Rissanen, *Angew. Chem., Int. Ed.*, 2000, **39**, 2504.
16 PLATON VOIDS probe diameter 1.2 Å, grid 0.2 Å, A. L. Spek, *J. Appl. Crystallogr.*, 2003, **36**, 7.
17 B. L. Schottel, H. T. Chifotides and K. R. Dunbar, *Acc. Chem. Res.*, 2007, **40**, 435.
18 P. Atkins and J. De Paula, *Physical Chemistry*, Oxford University Press, 8th edn, 2006, ch. 5; O. Kahn, *Molecular Magnetism*, VCH, 1993, 60.
19 H. Tokoro, S. Ohkoshi, T. Matsuda and K. A. Hashimoto, *Inorg. Chem.*, 2004, **43**, 5231.